Propagation of Rayleigh Waves in the Earth

Z. Alterman, H. Jarosch and C. L. Pekeris

"As when the massy substance of the Earth quivers."—*C. Marlowe, Tamburlaine the Great.* Pt. 2, I. 1.

Summary

The propagation of Rayleigh waves in the Earth is investigated in the whole range of periods T from about 10 s up to one hour. Three methods are necessary in order to cover this range of periods effectively. The standard *flat Earth method*, with neglect of gravity, gives values for the phase velocity C correct to within 1 per cent up to $T = 50$ s only, and for the group velocity U up to $T = 250$ s. The method of the *flattening of the Earth*, with neglect of gravity, has the 1 per cent accuracy limits for C and U at 300 and 400, respectively. Inclusion of gravity effects in the flattening of the Earth approximation does not alter the above limits. For $T > 300$ ($n < 25$) one must determine the period $T(n)$ of free oscillation of the Earth as a function of the order of the spherical harmonic n. This involves the solution of a system of differential equations of the sixth order, in which the gravitational effects are included. The wave penetrates appreciably into the core already at $T = 600$. Using the above three methods in their respective ranges of validity, we have evaluated $C(T)$ and $U(T)$ for (1) Bullen's Model B, (2) the Jeffreys–Bullen Model, as modified by Dorman, Ewing and Oliver, and (3) the Gutenberg Model. The observed Rayleigh group velocity data of Ewing and Press for $T < 380$ s and the phase velocity data of Nafe and Brune for $T < 300$ s agree with the values computed for the Gutenberg model, but not for the other models. This substantiates a previous conclusion reached by Takeuchi, Press and Kobayashi and by Dorman, Ewing and Oliver that the observed Rayleigh wave data provide evidence in support of Gutenberg's low-velocity layer. The few observed Rayleigh group velocities between $T = 400$ and 600 are substantially lower than the theoretical values for all the three models.

1. Introduction

In a previous investigation (Alterman, Jarosch & Pekeris 1959) subsequently referred to as I, methods were developed for determining the periods of free oscillation of the Earth as represented by models based on earthquake data and on other geophysical information concerning the internal constitution of the Earth. Our initial aim was to test a conjecture of Benioff (1954) that the 57-min oscillation which he observed on the records of the Kamchatka earthquake of 1952 is a free spheroidal oscillation of the Earth. This study, which dealt primarily with oscillations of spherical harmonic order $n = 2$, was then extended also to the dynamical theory of Earth tides (I, and Pekeris & others 1959). Recent advances (Benioff & Press 1958) made in the design of long-period seismographs hold out the hope of extending the observed seismic spectrum up to the one-hour limit. Already Ewing and Press (Benioff & Press 1958, and Ewing & Press 1956) have succeeded in recording Rayleigh waves of a period T of 630 s. The propagation of waves of periods of 600 s and higher is governed by the free modes of oscillation of the Earth of spherical harmonic order n ranging from 10 to 2. The amplitude of these modes extends from the surface of the Earth down into the core and their motion is governed not only by the elastic restoring forces but also by forces arising from the perturbed gravitational field. The analysis of these modes has therefore to be made by solving the systems of 6 differential equations I(28) to I(33) and I(35) to I(39) in the mantle and core respectively. This *complete normal mode method* must be used for periods $T > 400$ s, ($n < 17$). In the range of $400 > T > 300$ ($17 < n < 25$) the amplitude of the normal modes becomes negligibly small throughout the core, so that it is sufficient to carry out the integrations only from the bottom of the mantle to the surface. In this *restricted normal mode method* one imposes the condition at the core boundary of the vanishing of all of the components of the displacements, and of the stresses.

In the period-range of $300 > T > 50$ ($25 < n < 200$) the analysis can be considerably simplified by taking account of the approach to flat Earth conditions, without, however, altogether neglecting the still appreciable effect of the sphericity of the Earth. This is accomplished by the use of the *Earth-flattening approximation*. In this method the space metric is transformed so as to make the surface of the Earth flat and to curve rays which were originally straight. The effect of the sphericity of the Earth turns out to be equivalent to the superposition on the given velocity–depth function of a perturbation term which varies linearly with depth. In the period ranges where the Earth-flattening approximation applies we have found that the gravitational forces may be neglected.

Finally, for periods $T < 50$ s, the standard flat Earth approximation with neglect of gravity is valid. This method has been used extensively by Stoneley (1953), and recently by Press & Takeuchi (1960), and by Dorman, Ewing & Oliver (1960). The regions of applicability of the various methods are summarized in Table 1.

Table 1

Ranges of applicability of various methods

Range of period T in seconds	Range of n	Method	Core included	Gravity included
$3220 > T > 400$	$17 > n > 2$	Complete normal mode	Yes	Yes
$400 > T > 300$	$25 > n > 17$	Restricted normal mode	No	Yes
$300 > T > 50$	$200 > n > 25$	Earth flattening approximation	No	No
$50 > T$	$n > 200$	Flat earth	No	No

The limits set for the applicability of the various approximate methods were obtained by comparing results obtained for the phase velocity C with those derived from the complete normal mode theory. It turns out that the group velocities U come out more accurately by the approximate methods than do the phase velocities C.

We have carried out the analysis of propagation of Rayleigh waves in the Earth for three models whose properties are described in Tables 2, 3, and 4 and in Figures 1 and 2. The "Jeffreys–Bullen" Model is taken from a paper by Dorman, Ewing & Oliver (1960). In their method of calculation of dispersion of Rayleigh waves, the Earth is represented by a system of homogeneous layers. They have determined the properties of these layers so as to follow the average properties of the Jeffreys–Bullen Model. The "Bullen" Model is based on the data given (Bullen 1950) for Bullen's Model B, with linear interpolation at intermediate points. The properties of the top layer of 33 km thickness are taken from the paper by Press & Takeuchi (1960). The data on the step-function model designated as the "Gutenberg" Model are taken from the paper by Dorman, Ewing & Oliver (1960) and from Bullen's book *An Introduction to the Theory of Seismology*, p. 218. This model differs from the other two by having a *low-velocity layer*.

2. The normal mode solution

In studying the propagation of Rayleigh waves of periods $T > 300$ s we must follow the method of normal modes described in I. The periods of free spheroidal oscillations for Bullen's Model B were there given in Table 4 for $n = 2$, 3, and 4. We have extended this analysis to higher values of n, and the results are shown in Table 5 of the present paper. The direct result of the eigenvalue problem is the period $T(= 2\pi/\sigma)$ for a given value of n. The normal mode is then represented by a standing oscillation of the form

$$V = \exp(i\sigma t)F(r)P_n(\cos\theta). \tag{1}$$

Such a standing oscillation can be conceived as the result of a superposition of two waves travelling in opposite directions. For large n this decomposition can be accomplished by the use of the asymptotic expansion of $P_n(\cos\theta)$:

$$V \to F(r)(2n\pi\sin\theta)^{-\frac{1}{2}}\left\{\exp\left(i\left[\sigma t-(n+\tfrac{1}{2})\theta+\frac{\pi}{4}\right]\right)+ \right.$$
$$\left. +\exp\left(i\left[\sigma t+(n+\tfrac{1}{2})\theta-\frac{\pi}{4}\right]\right)+O(1/n)\right\}. \tag{2}$$

The first term in the braces represents a wave travelling in the positive θ-direction:

$$\sigma t-(n+\tfrac{1}{2})\theta = \sigma t-\frac{x}{C}, \tag{3}$$

$$x = a\theta, \qquad C = \frac{a\sigma}{(n+\frac{1}{2})}, \qquad k = \frac{\sigma}{C} = \frac{(n+\frac{1}{2})}{a}. \tag{4}$$

A group velocity U can be derived from

$$U = \frac{d(kC)}{dk} = a\frac{d\sigma}{dn}. \tag{5}$$

The values of U given in Table 5 were obtained by finite differencing of $\sigma(n)$. For

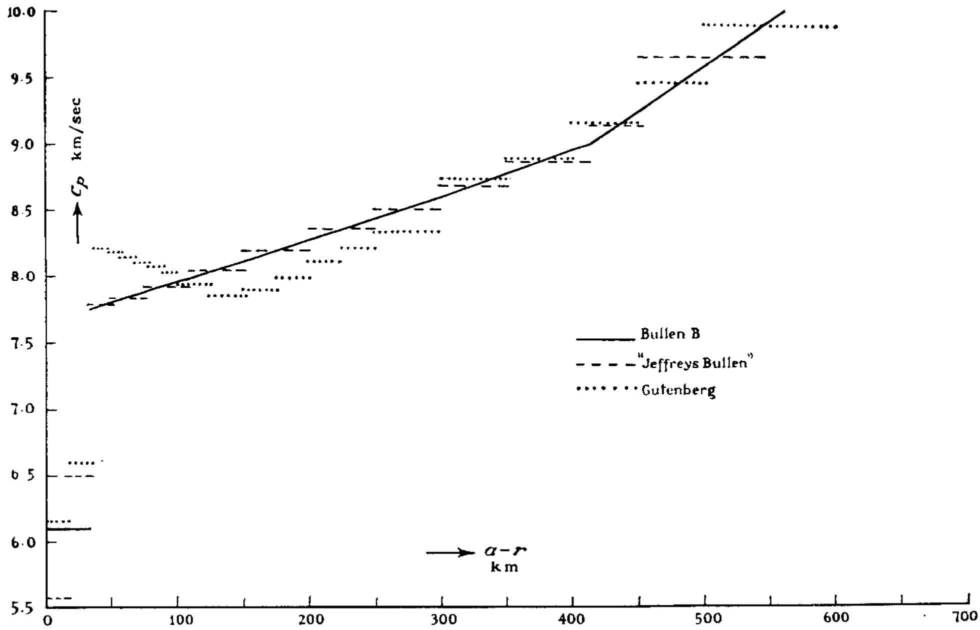

FIG. 1.—Variation with depth $a-r$ of the compressional velocity C_p for models Bullen B, "Jeffreys–Bullen" and Gutenberg.

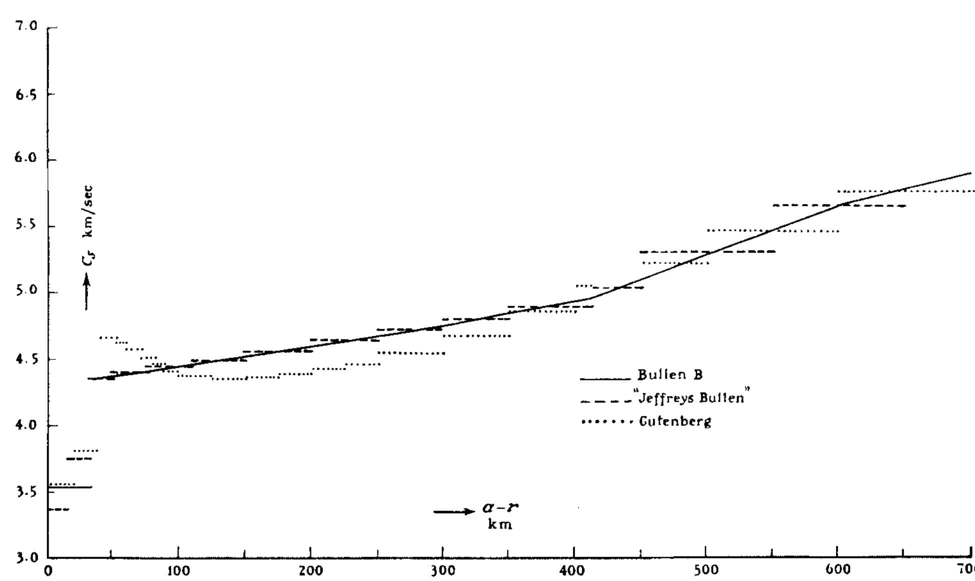

FIG. 2.—Variation with depth $a-r$ of the shear velocity C_s for models Bullen B, "Jeffreys–Bullen" and Gutenberg.

Table 2

Properties of the Bullen B Earth Model

$a-r$	ρ	C_p	C_s	μ	λ	g
km	g/cm^3	km/s	km/s	10^{11} dyn/cm^2	10^{11} dyn/cm^2	cm/s^2
0	2·76	6·10	3·54	3·45	3·37	982
33	2·82	6·10	3·54	3·52	3·45	985
33	3·32	7·75	4·35	6·28	7·38	985
80	3·36	7·89	4·42	6·56	7·77	986
80	3·87	7·89	4·42	7·56	8·95	986
100		7·95	4·45			
200	3·94	8·26	4·60	8·34	10·21	985
300		8·58	4·76			
400	4·06	8·93	4·94	9·90	12·55	983
413		8·97	4·96			
600	4·18	10·25	5·66	13·39	17·13	980
800	4·30	11·00	6·13	16·16	19·71	978
1 000	4·41	11·42	6·36	17·84	21·84	976
1 200	4·52	11·71	6·50	19·10	23·79	976
1 400	4·63	11·99	6·62	20·29	25·98	976
1 600	4·74	12·26	6·73	21·47	28·31	978
1 800	4·84	12·53	6·83	22·58	30·83	982
2 000	4·94	12·79	6·93	23·72	33·36	987
2 200	5·03	13·03	7·02	24·79	35·82	997
2 400	5·13	13·27	7·12	26·01	38·32	1 010
2 600	5·22	13·50	7·21	27·14	40·86	1 029
2 700	5·27	13·57	7·26	27·74	41·57	1 042
2 800		13·64	7·30			
2 898		13·64	7·30			
2 898		8·10				
2 900	5·57			29·68	44·26	1 069
2 900	9·74				63·94	1 069
3 000	9·90	8·22			66·89	1 041
3 200	10·20	8·47			73·18	1 006
3 400	10·47	8·76			80·34	960
3 600	10·72	9·04			87·61	913
3 800	10·95	9·28			94·30	865
4 000	11·16	9·51			100·93	815
4 200	11·36	9·70			106·89	765
4 400	11·54	9·88			112·65	718
4 600	11·71	10·06			118·51	670
4 800	11·87	10·25			124·71	628
4 982	12·00	10·44			130·79	599
5 121	15·00	9·47			134·52	563
5 121	15·00	11·16			186·82	563
5 700		11·26				
6 371	17·90	11·31			228·92	0

Table 3

Properties of Jeffreys–Bullen Earth Model as modified by Dorman, Ewing & Oliver (1960)

$a-r$ km	ρ g/cm³	C_p km/s	C_s km/s	μ 10^{11} dyn/cm²	λ 10^{11} dyn/cm²
0					
	2·65	5·57	3·36	2·99	2·24
15					
	2·87	6·50	3·74	4·01	4·10
33					
	3·33	7·78	4·36	6·33	7·47
50					
	3·35	7·83	4·39	6·46	7·63
75					
	3·37	7·92	4·44	6·64	7·85
110					
	3·41	8·04	4·49	6·87	8·29
150					
	3·45	8·19	4·56	7·17	8·79
200					
	3·49	8·35	4·64	7·51	9·31
250					
	3·53	8·50	4·72	7·86	9·78
300					
	3·57	8·67	4·80	8·23	10·38
350					
	3·62	8·86	4·90	8·68	11·02
413					
	3·70	9·14	5·04	9·40	12·11
450					
	3·89	9·65	5·31	10·97	14·29
550					
	4·13	10·25	5·66	13·21	16·91
650					
	4·32	10·68	5·93	15·19	18·89
750					
	4·49	11·00	6·13	16·87	20·58
850					
	4·62	11·28	6·29	18·28	22·23
1 000					
	4·74	11·57	6·44	19·65	24·13
1 200					
	4·92	11·99	6·62	21·54	27·58
1 600					
	5·14	12·53	6·83	23·95	32·71
2 000					
	5·34	13·03	7·02	26·32	38·03
2 400					
	5·54	13·50	7·21	28·80	43·37
2 800					
	5·69	13·64	7·30	30·32	45·22

Table 4

Properties of the Gutenberg Earth Model

$a-r$ km	ρ g/cm³	C_p km/s	C_s km/s	μ 10^{11} dyn/cm²	λ 10^{11} dyn/cm²	g cm/s²
0						
	2·74	6·14	3·55	3·45	3·42	982
19						
	3·00	6·58	3·80	4·33	4·32	983
38						
	3·32	8·20	4·65	7·18	7·97	984
50						
	3·34	8·17	4·62	7·13	8·04	985
60						
	3·35	8·14	4·57	7·00	8·20	985
70						
	3·36	8·10	4·51	6·83	8·38	986
80						
	3·37	8·07	4·46	6·70	8·54	986
90						
	3·38	8·02	4·41	6·57	8·59	986
100						
	3·39	7·93	4·37	6·47	8·37	986
125						
	3·41	7·85	4·35	6·45	8·11	987
150						
	3·43	7·89	4·36	6·52	8·31	988
175						
	3·46	7·98	4·38	6·64	8·76	989
200						
	3·48	8·10	4·42	6·80	9·23	989
225						
	3·50	8·21	4·46	6·96	9·67	990
250						
	3·53	8·38	4·54	7·28	10·24	991
300						
	3·58	8·62	4·68	7·84	10·92	992
350						
	3·62	8·87	4·85	8·52	11·45	993
400						
	3·69	9·15	5·04	9·37	12·15	995
450						
	3·82	9·45	5·21	10·37	13·38	996
500						
	4·01	9·88	5·45	11·91	15·32	997
600						
	4·21	10·30	5·76	13·97	16·73	998
700						
	4·40	10·71	6·03	16·00	18·47	998
800						
	4·56	11·10	6·23	17·70	20·79	997
900						
	4·63	11·35	6·32	18·49	22·66	995
1 000						
	4·74	11·60	6·42	19·54	24·71	993
1 200						
	4·85	11·93	6·55	20·81	27·41	990
1 400						
	4·96	12·17	6·69	22·20	29·06	986

P

Table 4—*continued*

$a-r$	ρ	C_p	C_s	μ	λ	g
km	g/cm^3	km/s	km/s	10^{11} dyn/cm^2	10^{11} dyn/cm^2	cm/s^2
	4·96	12·17	6·69	22·20	29·06	986
1 600						
	5·07	12·43	6·80	23·44	31·45	983
1 800						
	5·19	12·67	6·90	24·71	33·90	982
2 000						
	5·29	12·90	6·97	25·70	36·63	981
2 200						
	5·39	13·10	7·05	26·79	38·92	984
2 400						
	5·49	13·32	7·15	28·07	41·27	989
2 600						
	5·59	13·59	7·23	29·22	44·80	997
2 800						
	5·69	13·70	7·20	29·50	47·80	1 011
2 898	9·40	8·10			61·71	1 037
3 000	9·55	8·23			64·72	1 015
3 500	10·15	8·90			80·42	908
4 000	10·7	9·50			96·58	800
4 500	11·2	9·97			111·39	631
4 982	11·5	10·44			125·34	469
5 121	12·0	10·75			138·66	422
6 371	12·3	11·31			157·34	0

small values of n, of course, the expansion (2) is not valid and the usual concept of group-velocity requires modification. The distribution of amplitude with depth in the normal modes is shown in Figures 3 to 6. It is seen that for $n = 10$ ($T = 591$) the amplitude in the core is still appreciable. On the other hand, for $n > 17$ the amplitude in the core becomes negligibly small, and we may confine the integration to the mantle.

3. The Earth flattening approximation

For periods around 300 s the amplitude of the free oscillations is not only negligibly small in the core but also in the lower part of the mantle. It is, however, still not permissible to neglect altogether the curvature of the Earth. Referring to Figure 7, the sphericity of the Earth makes itself felt through the circumstance that a pulse originating on the surface at the point A can reach a point C sooner by travelling along the chord ADC rather than along the arc ABC. The flattening of the Earth approximation (Pekeris 1946; Pryce 1953; Koo & Katzin 1960) transforms the problem of propagation over a sphere to one over a flat Earth while still retaining the features of the inherent geometry of the sphere. This is accomplished by transforming the space-metric so as to make the surface flat and the rays curved. If the travel time along the ray ADC in the transformed flat space of Figure 7 is to be

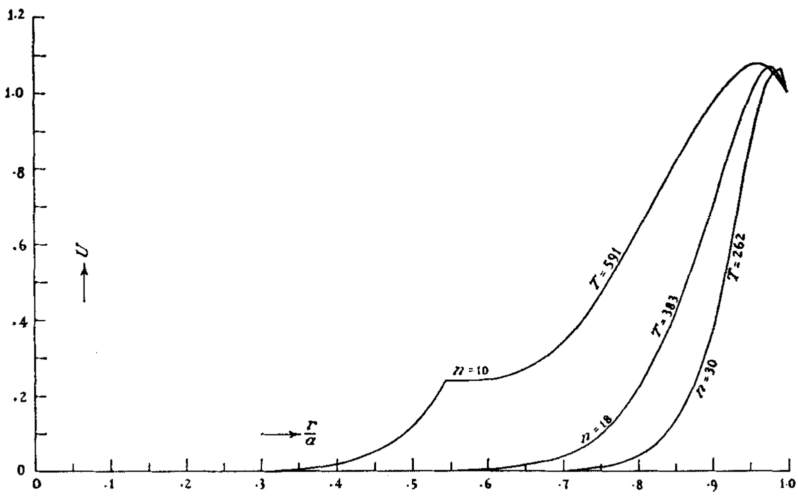

FIG. 3.—Distribution of radial displacement U in the normal spheroidal modes of orders $n = 10$, 18, and 30 in model Bullen B.

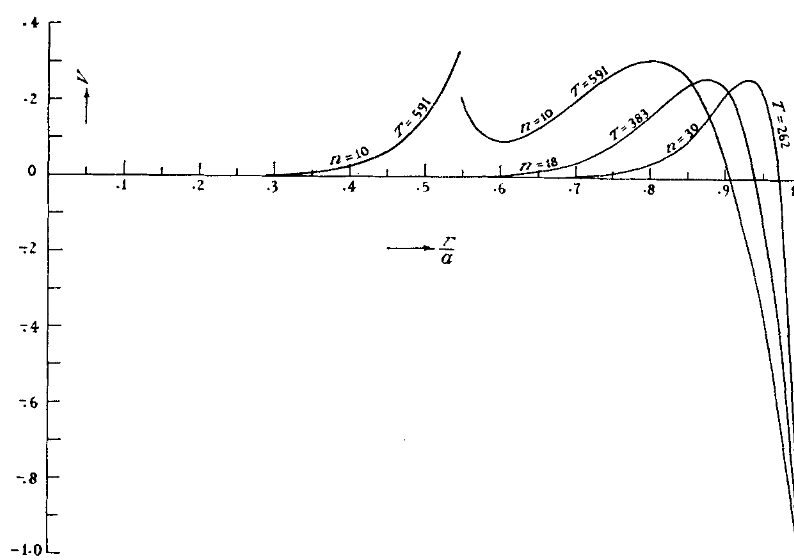

FIG. 4.—Distribution of horizontal displacement V in the normal spheroidal modes of orders $n = 10$, 18 and 30 in model Bullen B.

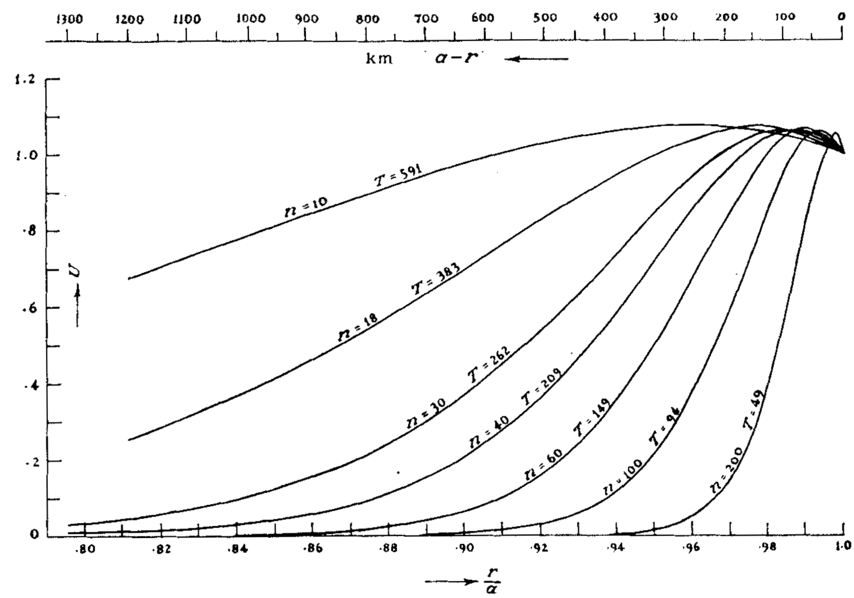

FIG. 5.—Distribution of radial displacement U in the normal spheroidal modes of orders n = 10 to 200 in model Bullen B.

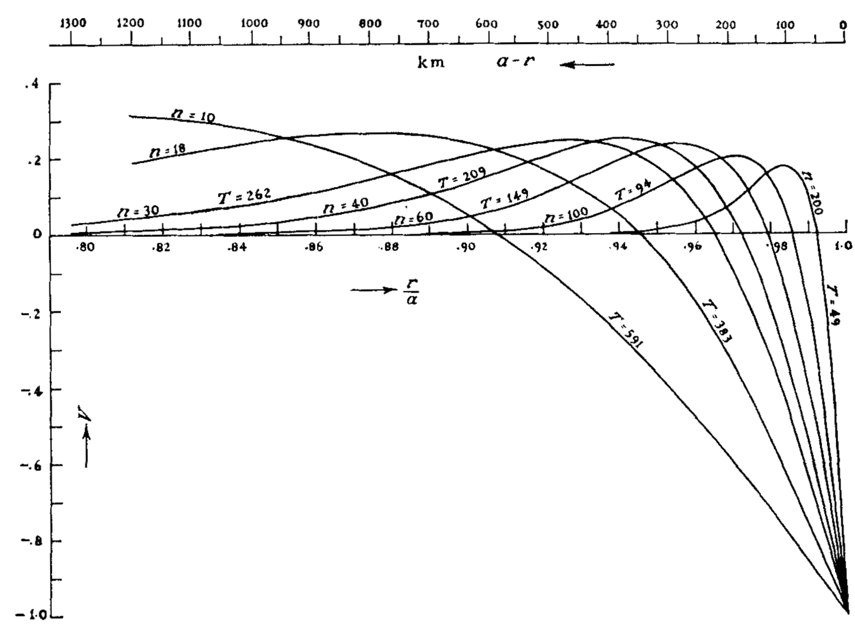

FIG. 6.—Distribution of horizontal displacement V in the normal spheroidal modes of orders n = 10 to 200 in model Bullen B.

less than along the ray ABC, then the velocity must increase with depth. The amount of this velocity variation with depth can be established from the form which the differential equations for the sphere take on for large values of n. The procedure can be demonstrated most directly for the free torsional oscillations.

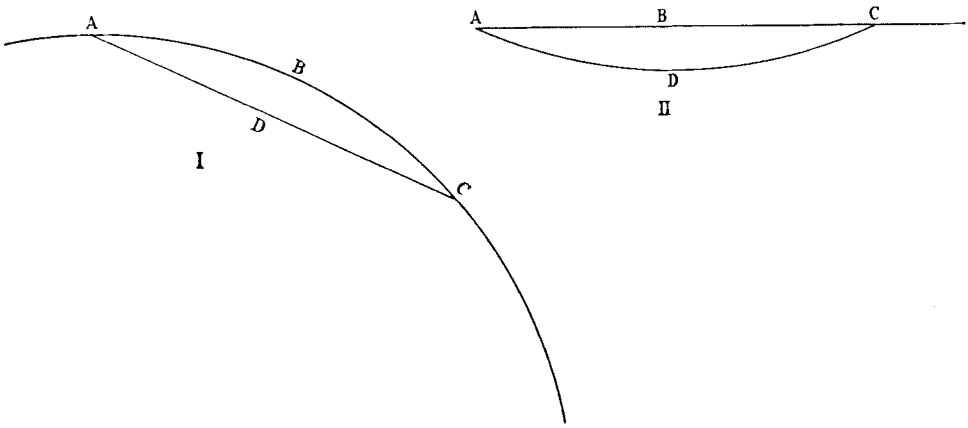

FIG. 7.—The flattening of the Earth approximation.

In that case the radial component of motion u vanishes, and the horizontal components v and w are derived from one function ψ

$$v = \frac{1}{\sin\theta}\frac{\partial\psi}{\partial\phi}\exp(i\sigma t), \qquad w = -\frac{\partial\psi}{\partial\theta}\exp(i\sigma t), \tag{6}$$

which obeys the differential equation

$$\frac{\partial^2\psi}{\partial r^2}+\frac{2}{r}\frac{\partial\psi}{\partial r}+\frac{1}{\mu}\frac{d\mu}{dr}\left(\frac{\partial\psi}{\partial r}-\frac{\psi}{r}\right)+\left[\frac{\sigma^2}{c^2}-\frac{1}{r^2}\left(\frac{\partial^2\psi}{\partial\theta^2}+\frac{\cos\theta}{\sin\theta}\frac{\partial\psi}{\partial\theta}+\frac{1}{\sin^2\theta}\frac{\partial^2\psi}{\partial\phi^2}\right)\right] = 0, \tag{7}$$

where c denotes the shear velocity:

$$c^2 = \mu/\rho_0. \tag{8}$$

Putting now

$$\psi(r,\theta,\phi) = U(r)P(\theta)\exp(im\phi), \tag{9}$$

we get

$$\frac{d^2P}{d\theta^2}+\frac{\cos\theta}{\sin\theta}\frac{dP}{d\theta}-\frac{m^2}{\sin^2\theta}P+a^2k^2P = 0, \tag{10}$$

$$\frac{d^2U}{dr^2}+\frac{2}{r}\frac{dU}{dr}+\frac{1}{\mu}\frac{d\mu}{dr}\left(\frac{dU}{dr}-\frac{U}{r}\right)+\left(\frac{\sigma^2}{c^2}-\frac{a^2k^2}{r^2}\right)U = 0. \tag{11}$$

Here a denotes the radius of the Earth, and we have written a^2k^2 instead of the customary separation constant $n(n+1)$ with the intention of relinquishing the requirement that P be finite at $\theta = 0$ and $\theta = \pi$. The plan is to build up a solution satisfying the source-condition and the outgoing wave condition from a series which converges rapidly everywhere except near the points $\theta = 0$, and $\theta = \pi$, where each term of the series becomes singular. The limiting form of equations

(10) and (11) as $ak \to \infty$ is obtained by using as horizontal and vertical coordinates

$$x = a\theta, \qquad h = a - r, \tag{12}$$

and neglecting terms of order $1/a$, except when they are multiplied by the large factor k^2:

$$\frac{d^2P}{dx^2}+\frac{1}{x}\frac{dP}{dx}+\left(k^2-\frac{m^2}{x^2}\right)P = 0 \tag{13}$$

$$\frac{d^2U}{dh^2}+\frac{1}{\mu}\frac{d\mu}{dh}\frac{dU}{dh}+\left[\frac{\sigma^2}{c^2}-k^2\left(1+2\frac{h}{a}\right)\right]U = 0. \tag{14}$$

The appropriate form for ψ in (9) is now

$$\psi = U(h)H_m^{(2)}(kx)\exp(im\phi), \tag{15}$$

where $H_m^{(2)}(kx)$ denotes the Hankel function of the second kind, and U is a solution of equation (14). For given functions $c(h)$ and $\mu(h)$ the boundary value problem (14) determines the frequency σ as a function of the wave number k, thus establishing the dispersion relation for Love waves.

Equation (14) resembles the equation for the propagation of Love waves on a flat Earth, except for the factor $[1+2(h/a)]$ which arises from the curvature of the Earth. Now since $k \simeq (\sigma/c_0)$, we have

$$\frac{\sigma^2}{c^2}-2k^2\frac{h}{a} \simeq \frac{\sigma^2}{\{c[1+(h/a)]\}^2}. \tag{16}$$

The flattening of the Earth approximation thus effectively introduces a linear increase of velocity with depth.

In the case of spheroidal oscillations, the modifications of equations I(28) to I(33), which are introduced by the Earth flattening approximation, can be derived simply by writing

$$u = \frac{\partial\psi}{\partial r}+\frac{1}{r^2\sin\theta}\frac{\partial\Omega}{\partial\theta}, \qquad v = \frac{1}{r}\frac{\partial\psi}{\partial\theta}-\frac{1}{r\sin\theta}\frac{\partial\Omega}{\partial r}, \qquad w = 0, \tag{17}$$

$$\psi = F(r)P_n(\theta), \qquad \Omega = H(r)\sin\theta\frac{\partial P_n}{\partial\theta}. \tag{18}$$

It is then found that the functions $U(r)$ and $V(r)$ of equations I(26) and I(27) are given by

$$U(r) = \frac{dF}{dr}-\frac{n(n+1)}{r^2}H, \tag{19}$$

$$V(r) = \frac{1}{r}\left(F-\frac{dH}{dr}\right). \tag{20}$$

When (19) and (20) are substituted into equations I(28) to I(33) the flattening of the Earth approximation is effected by writing

$$\frac{n(n+1)}{r^2} \to k^2\left(1+\frac{2h}{a}\right). \tag{21}$$

The same result can, however, be obtained directly from I(28) to I(33) by using as variables ry_3 and ry_4 instead of y_3 and y_4, as is suggested by the $1/r$ factor in (20).

We thus get

$$-\frac{dy_1}{dh} = \frac{y_2}{(\lambda+2\mu)} + \frac{\lambda}{(\lambda+2\mu)}k^2\left(1+\frac{2h}{a}\right)(ry_3) \tag{22}$$

$$-\frac{dy_2}{dh} = -\sigma^2\rho y_1 + k^2\left(1+2\frac{h}{a}\right)[\rho g(ry_3)+(ry_4)] - \rho y_4, \tag{23}$$

$$-\frac{d(ry_3)}{dh} = -y_1 + \frac{(ry_4)}{\mu}, \tag{24}$$

$$-\frac{d(ry_4)}{dh} = g\rho y_1 - \frac{\lambda y_2}{(\lambda+2\mu)} + \left[-\rho\sigma^2 + \frac{4\mu(\lambda+\mu)}{(\lambda+2\mu)}k^2\left(1+2\frac{h}{a}\right)\right](ry_3) - \rho y_5, \tag{25}$$

$$-\frac{dy_5}{dh} = 4\pi G\rho y_1 + y_6, \tag{26}$$

$$-\frac{dy_6}{dh} = -4\pi G\rho k^2\left(1+\frac{2h}{a}\right)(ry_3) + k^2\left(1+\frac{2h}{a}\right)y_5. \tag{27}$$

It is convenient to put these equations in non-dimensional form. Let λ^* denote the maximum value of λ in the Earth,

$$\lambda = \lambda^*\lambda_1 \qquad \mu = \lambda^*\mu_1, \qquad g = g(a)g_1, \tag{28}$$

$$\rho = \bar{\rho}\rho_1, \qquad b = \frac{\bar{\rho}\sigma^2a^2}{\lambda^*}, \qquad c = \frac{\bar{\rho}^2a^2C}{\lambda^*}, \tag{29}$$

$$y_1 = az_1, \qquad y_2 = \lambda^*z_2 \qquad ry_3 = a^2z_3, \tag{30}$$

$$ry_4 = a\lambda^*z_4, \qquad y_5 = a^2C\bar{\rho}z_5, \qquad y = aC\bar{\rho}z_6. \tag{31}$$

$$n(n+1) = a^2k^2 \qquad s = r/a.$$

Equations (22) to (27) then become

$$\frac{dz_1}{ds} = \frac{z_2}{(\lambda_1+2\mu_1)} + \frac{\lambda_1}{(\lambda_1+2\mu_1)}n(n+1)\left(1+\frac{2h}{a}\right)z_3, \tag{33}$$

$$\frac{dz_2}{ds} = -b\rho_1z_1 + n(n+1)\left(1+\frac{2h}{a}\right)\left[\frac{4\pi}{3}c\rho_1g_1z_3 + z_4\right] - c\rho_1z_6, \tag{34}$$

$$\frac{dz_3}{ds} = -z_1 + \frac{z_4}{\mu_1}, \tag{35}$$

$$\frac{dz_4}{ds} = \frac{4\pi}{3}cg_1\rho_1z_1 - \frac{\lambda_1}{(\lambda_1+2\mu_1)}z_2 - b\rho_1z_3 + \frac{4\mu_1(\lambda_1+\mu_1)}{(\lambda_1+2\mu_1)}n(n+1)\left(1+2\frac{h}{a}\right)z_3 - c\rho_1z_5, \tag{36}$$

$$\frac{dz_5}{ds} = 4\pi\rho_1z_1 + z_6, \tag{37}$$

$$\frac{dz_6}{ds} = -4\pi n(n+1)\left(1+\frac{2h}{a}\right)\rho_1z_3 + n(n+1)\left(1+\frac{2h}{a}\right)z_5. \tag{38}$$

The boundary condition at the surface of the Earth $r = a$ is

$$z_2 = 0, \qquad z_4 = 0, \qquad z_6 + (n+1)z_5 = 0. \tag{39}$$

At the boundary of the core we require the vanishing of all the z_i.

4. Discussion of results

Our results for the dispersion of Rayleigh waves in the Earth are given in Tables 5, 6 and 7 and in Figures 8 and 9 for Bullen's Model B; in Table 8 and Figure 10 for the "Jeffreys–Bullen" Model; and in Tables 9, 10 and 11 and Figure 11 for the Gutenberg Model. The regions of applicability of the various methods of approximation can be judged from the results for Bullen's Model B shown in Figure 8. The phase velocity curve C (dashed) and the group velocity curve U of the Earth flattening approximation begin to deviate from the exact normal mode curve (solid) at about $T = 250$ s, while the plane Earth curve (dotted) for C is in error already beyond $T = 40$ s. The group velocity curve U for the plane Earth approximation turns out to be accurate up to about 250 s. Inclusion

Table 5

Period T, phase velocity C and group velocity U for Bullen's Model B obtained by the normal mode solution. The interpolation is based on the exact values, computed at intervals of 5. n denotes the order of spherical harmonic. For n < 17 the solution extends through the mantle and core; for n > 17 the amplitude in the core is negligible.

n	T min Exact	T min Interpol.	C km/s	U km/s	n	T min Exact	T min Interpol.	C km/s	U km/s
2	53·70		4·97		32		4·16	4·94	
3	35·50		5·37	6·75	33		4·06	4·91	
4	25·73		5·76	7·41	34		3·97	4·88	
5	19·85		6·11	7·73	35	3·88		4·85	
6	16·12		6·37	7·64	36		3·79	4·82	
7	13·64		6·52	7·20	37		3·71	4·80	
8	11·95		6·57	6·53	38		3·63	4·77	
9	10·77		6·52	5·85	39		3·56	4·75	
10	9·88		6·43	5·33	40	3·49		4·73	
11	9·18	9·16	6·32	5·01			3·45		3·84
12	8·61	8·57	6·20	4·80	41	3·42	3·42	4·70	
13	8·11	8·08	6·09	4·66	42		3·35	4·68	
14	7·68	7·67	5·99	4·56	43		3·29	4·66	
15	7·30		5·89	4·48	44		3·23	4·65	
16	6·96	6·97	5·81	4·40	45	3·17		4·63	
17	6·66	6·66	5·72	4·33	46		3·11	4·61	
18	6·39	6·39	5·65	4·27	47		3·06	4·60	
19	6·14	6·14	5·57	4·21	48		3·00	4·58	
20	5·91		5·51	4·16	49		2·95	4·57	
21	5·70	5·69	5·44		50	2·90		4·55	3·87
22		5·48	5·41		51		2·85	4·54	
23		5·29	5·37		52		2·81	4·53	
24		5·12	5·32		53		2·76	4·51	
25	4·96		5·28		54		2·72	4·50	
26		4·82	5·22		55	2·68		4·49	3·88
27		4·70	5·16		56		2·64	4·48	
28		4·58	5·11		57		2·60	4·47	
29		4·47	5·06		58		2·56	4·46	
30	4·37		5·01		59		2·52	4·45	
		4·31		3·88	60	2·48		4·44	
31	4·26	4·26	4·98				2·47		3·89
					61	2·45	2·45	4·43	

Table 6

Earth flattening approximation for Bullen's Model B
σ—frequency, T—period, C—phase velocity, U—group velocity
$n(n+1) = a^2k^2$

n	σ	T	C	U
	s^{-1}	s	km/s	km/s
10	0·0106909	588	6·49	
		565		5·63
11	0·0115744	543	6·41	
12	0·0124334	505	6·34	
		490		4·98
13	0·0132144	475	6·24	
15	0·0146324	429	6·01	
		420		4·50
16	0·0153382	410	5·92	
20	0·0180421	348	5·61	
		342		4·16
21	0·0186946	336	5·54	
25	0·0211656	297	5·29	
		292		4·11
26	0·0218111	288	5·24	
30	0·0243188	258	5·08	
		255		3·88
31	0·0249272	252	5·04	
40	0·0303591	207	4·78	
		205		3·84
41	0·0309614	203	4·75	
60	0·0424755	148	4·47	
		147		3·89
61	0·0430858	146	4·46	
100	0·0670392	94	4·25	
		93		3·92
101	0·0676538	93	4·25	
150	0·0975178	64	4·13	
		64		3·84

n	σ	T	C	U
	s^{-1}	s	km/s	km/s
151	0·0981202	64	4·13	
200	0·127154	49	4·04	
		49		3·71
201	0·127736	49	4·04	
250	0·155644	40	3·96	
		40		3·55
252	0·156757	40	3·96	
300	0·182878	34	3·88	
		34		3·39
302	0·183941	34	3·87	
400	0·233856	27	3·72	
		27		3·12
402	0·234835	27	3·72	
500	0·281569	22	3·58	
		22		2·98
504	0·283439	22	3·58	
600	0·327989	19	3·48	
		19		2·95
604	0·329841	19	3·48	
806	0·424479	15	3·35	
		15		3·03
808	0·425431	15	3·35	
1 000	0·518212	12	3·30	
		12		3·12
1 003	0·519681	12	3·30	
		12		3·12
1 005	0·520661	12	3·30	

Table 7

Plane Earth approximation for Bullen Model B
σ—frequency, T—period, C—phase velocity, U—group velocity
$n(n+1) = a^2k^2$

n	σ	T	C	U
	s^{-1}	s	km/s	km/s
10	0·00890939	705	5·41	
		670		6·20
11	0·00988325	636	5·48	
		608		5·99
12	0·01082315	581	5·52	
		558		5·72
13	0·01172077	536	5·53	
15	0·01337545	469	5·50	
		457		4·87
16	0·01413967	444	5·46	
		433		4·67
17	0·01487227	422	5·41	
20	0·01694783	371	5·27	
		364		4·24
21	0·01761293	357	5·22	
		350		4·18
22	0·01826859	344	5·17	
25	0·02017568	311	5·04	
		307		4·04
26	0·02081038	302	5·00	
30	0·02329257	270	4·87	
		266		3·89
31	0·02390364	263	4·83	
40	0·02932744	214	4·61	
		212		3·82
41	0·02992771	210	4·59	
60	0·04136692	152	4·36	
		151		3·86
61	0·04197302	150	4·35	
100	0·06580556	95	4·17	
		95		3·90
101	0·06641823	95	4·17	
200	0·1258999	50	4·00	
		50		3·71
201	0·1264826	50	4·00	

Table 8

Earth flattening approximation for Jeffreys–Bullen Model.
σ—frequency, T—period, C—phase velocity, U—group velocity
$n(n+1) = a^2k^2$

n	σ	T	C	U
	s^{-1}	s	km/s	km/s
15	0·0150400	418	6·18	
		408		4·62
16	0·0157654	399	6·09	
20	0·0184944	340	5·75	
		334		4·15
21	0·0191461	328	5·67	
30	0·0246208	255	5·14	
		252		3·76
31	0·0252110	249	5·10	
40	0·0304432	206	4·79	
		204		3·69
41	0·0310228	203	4·76	
60	0·0421465	149	4·44	
		148		3·77
61	0·0427380	147	4·43	
100	0·0660051	95	4·18	
		94		3·81
102	0·0672006	93	4·18	
200	0·125091	50	3·97	
		50		3·70
201	0·125672	50	3·97	
400	0·234692	27	3·73	
		27		3·25
402	0·235712	27	3·73	
600	0·331074	19	3·51	
		19		2·96
604	0·332931	19	3·51	

Table 9

Period T, phase velocity C and group velocity U for Gutenberg Model obtained by the normal mode solution. n denotes the order of spherical harmonic. The interpolation is based on the exact values, computed at intervals of 5. For $n < 17$, the solution extends through the mantle and core; for $n > 17$ the amplitude in the core is negligible.

	T min		*C*	*U*		*T* min		*C*	*U*
n	Exact	Interpol.	km/s	km/s	*n*	Exact	Interpol.	km/s	km/s
2	53.52		4.99		33		4.06	4.91	
3	35.33		5.40	6.82	34		3.97	4.87	
4	25.54		5.80	7.52	35	3.89		4.84	
5	19.66		6.17	7.89	36		3.81	4.80	
6	15.92		6.45	7.85	37		3.73	4.77	
7	13.44		6.62	7.47	38		3.66	4.74	
8	11.74		6.69	6.84	39		3.59	4.71	
9	10.54		6.66	6.16	40	3.52		4.68	
10	9.65		6.59	5.61			3.49		3.58
11	8.95	8.93	6.48	5.23	41	3.45	3.45	4.65	
12	8.38	8.35	6.37	4.97	42		3.39	4.63	
13	7.90	7.87	6.26	4.80	43		3.33	4.61	
14	7.48	7.46	6.15	4.67	44		3.27	4.58	
15	7.11		6.05	4.56	45	3.22		4.56	
16	6.78	6.78	5.96	4.46	46		3.16	4.54	
17	6.49	6.49	5.87	4.35	47		3.11	4.52	
18	6.23	6.23	5.79	4.26	48		3.06	4.50	
19	6.00	6.00	5.71	4.17	49		3.01	4.48	
20	5.78		5.63	4.09	50	2.96		4.46	3.61
21	5.59	5.59	5.56		51		2.91	4.45	
22		5.40	5.49		52		2.87	4.43	
23		5.24	5.42		53		2.82	4.42	
24	5.08	5.08	5.36		54		2.78	4.40	
		5.01		3.82	55	2.74		4.39	3.66
25	4.94		5.30		56		2.70	4.38	
26		4.81	5.24		57		2.66	4.36	
27		4.68	5.18		58		2.62	4.35	
28		4.56	5.13		59		2.58	4.34	
29		4.45	5.08		60	2.55		4.33	
30	4.34		5.04				2.53		3.67
	4.29			3.64	61	2.51		4.32	
31	4.24	4.24	4.99						
32		4.15	4.95						

Table 10

Earth flattening approximation for Gutenberg Model
σ—frequency, T—period, C—phase velocity, U—group velocity
$n(n+1) = a^2k^2$

n	σ s^{-1}	T s	C km/s	U km/s
10	0·0112644	558	6·83	
		535		6·52
11	0·0122873	511	6·81	
		494		5·81
12	0·0131994	476	6·73	
		462		5·19
13	0·0140140	448	6·61	
		437		4·73
14	0·0147563	426	6·48	
		416		4·42
15	0·0154503	407	6·35	
		398		4·22
16	0·0161131	390	6·22	
20	0·0186168	338	5·79	
		332		3·86
21	0·0192227	327	5·70	
30	0·0244724	257	5·11	
		254		3·62
31	0·0250403	251	5·06	
40	0·0300884	209	4·73	
		207		3·57
41	0·0306482	205	4·71	
60	0·0414016	152	4·36	
		151		3·66
61	0·0419763	150	4·35	
100	0·0649582	97	4·12	
		96		3·34
101	0·0655616	96	4·12	
200	0·126078	50	4·01	
		50		3·89
201	0·126689	50	4·01	

Table 11

Plane Earth approximation for Gutenberg Model
σ—frequency, T—period, C—phase velocity, U—group velocity
$n(n+1) = a^2k^2$

n	σ s^{-1}	T s	C km/s	U km/s
12	0·0112840	557	5·75	
		539		6·30
13	0·0122726	512	5·79	
		494		5·97
14	0·0132103	476	5·80	
		461		5·57
15	0·0140852	446	5·79	
		434		4·75
16	0·0148923	422	5·75	
		411		3·95
17	0·0156372	401	5·69	
20	0·0176298	356	5·48	
		350		3·95
21	0·0182502	344	5·41	
25	0·0206441	304	5·16	
		300		3·73
26	0·0212293	296	5·10	

of gravitational forces in the Earth flattening approximation makes but a small improvement, as shown by the points ⊙.

A comparison of the theoretical group velocity curves of Rayleigh waves for various models with the observations of Ewing & Press (1956) is shown in Figures 9, 10 and 11. The theoretical group velocity curves for Bullen's Model B, as well as for the "Jeffreys–Bullen" Model, shown in Figures 9 and 10, are distinctly higher than the observed values for periods greater than 50 s. On the other hand, the theoretical group velocity curve for the Gutenberg Model agrees with the observations for periods up to about 380 s. This agreement can be taken as evidence in favour of Gutenberg's low-velocity layer as was first demonstrated by Takeuchi, Press & Kabayashi (1959), and by Dorman, Ewing & Oliver (1960).

The few observed Rayleigh wave group velocities in the high-period region of 400 to about 630 s are much lower than the theoretical values for all the three models. It would be interesting to substantiate this by further observations. The observed phase velocities C of Nafe and Brune shown in Figure 11 agree very well with the theoretical normal mode solution for $T < 300$. For $T > 300$ s, the observed C values are higher than the theoretical.

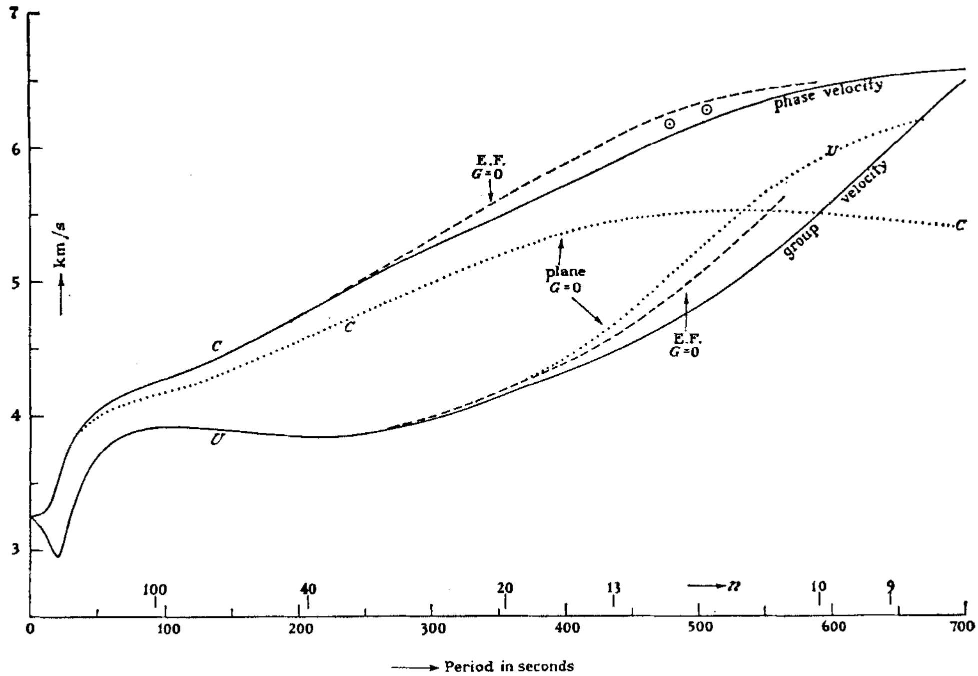

FIG. 8.—Group velocity U and phase velocity C for Bullen's model B. ——— exact normal mode theory, – – – – Earth flattening approximation with neglect of gravity, ... plane Earth with neglect of gravity, ⊙ Earth flattening approximation with gravity included.

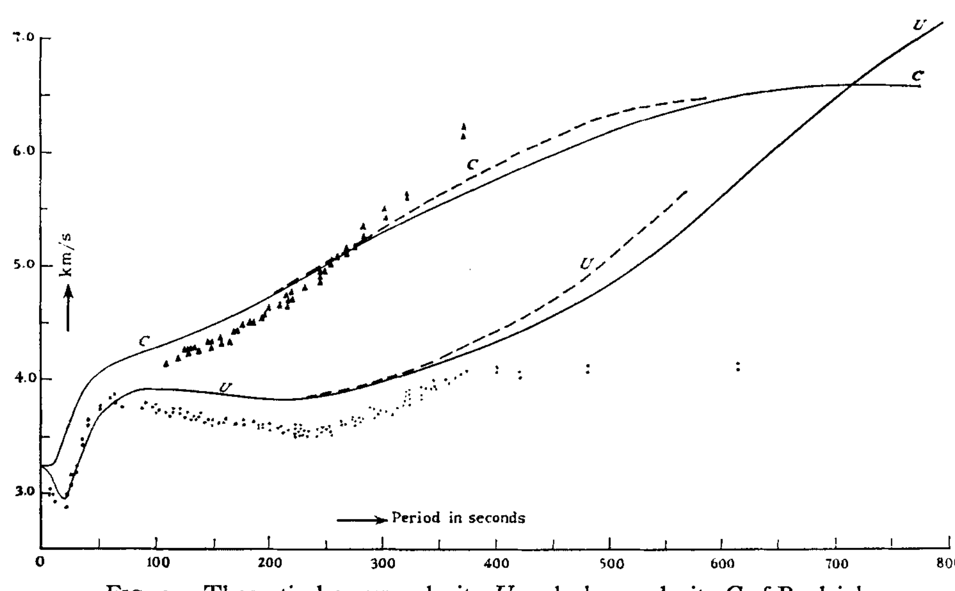

FIG. 9.—Theoretical group velocity U and phase velocity C of Rayleigh waves for Bullen's model. The dots are Rayleigh wave group velocities observed by Ewing & Press (1956). ——— normal mode solution, – – – – – Earth flattening approximation. The triangles are phase velocities observed by Nafe & Brune (1960).

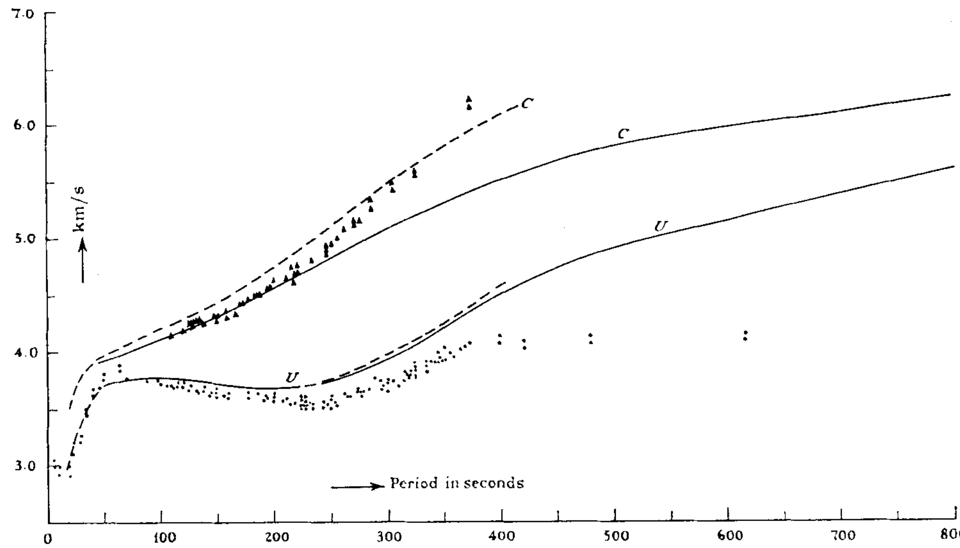

FIG. 10.—Theoretical phase velocity C and group velocity U of Rayleigh waves for the "Jeffreys–Bullen" model. The dots are Rayleigh group velocities observed by Ewing & Press (1956) – – – – – Earth flattening approximation. The triangles are phase velocities observed by Nafe & Brune (1960).

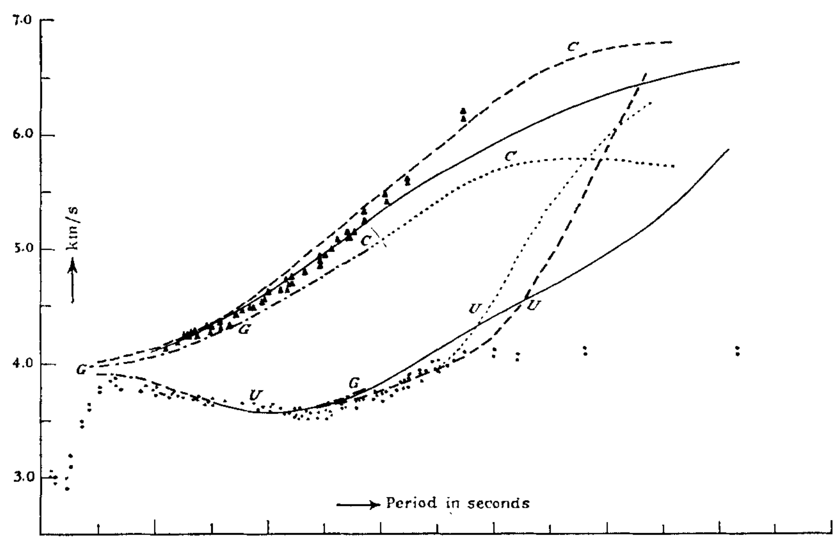

FIG. 11.—Theoretical phase velocity C and group velocity U of Rayleigh waves for Gutenberg Model. The dots are Rayleigh group velocities observed by Ewing & Press (1956). Curves G were computed by Dorman, Ewing & Oliver. – – – – – Earth flattening approximation, ... Plane Earth approximation, ——— Normal mode solution. The triangles are phase velocities observed by Nafe & Brune (1960).

Weizmann Institute of Science,
Rehovot,
Israel:

1960 *September*

References

Alterman, Z., Jarosch, H. & Pekeris, C. L., 1959. *Proc. Roy. Soc. A*, **252**, 80.
Benioff, H., 1954. *Trans. Amer. Geophys. Un.*, **35**, 985.
Benioff, H. & Press, F., 1958. *Geophys. J.*, **1**, 208.
Bullen, K. E., 1950. *Mon. Not. R. Astr. Soc. Geophys. Suppl.*, **6**, 50.
Dorman, J., Ewing, M. & Oliver, J., 1960. *Bull. Seismol. Soc. Amer.*, **50**, 87.
Ewing, M. & Press, F., 1956. *Trans. Amer. Geophys. Un.*, **37**, 213.
Koo, Y. C. & Katzin, M., 1960. *Jour. Res. Nat. Bur. Stand.*, **64D.**, 61.
Nafe, J. E. & Brune, J. N., 1960. *Bull. Seismol. Soc. Amer.*, **50**, July.
(In a forthcoming publication the authors re-analyse their data and arrive at lower values for the phase velocity. The reduction amounts to about 1 per cent at a period of 200 s and increases to about 3 per cent at a period of 400 s.)
Pekeris, C. L., 1946. *Phys. Rev.*, **70**, 518.
Pekeris, C. L., Jarosch, H. & Alterman, Z., 1959. *Proceedings, Third International Symposium on Earth Tides, Trieste.*
Press, F. & Takeuchi, H., 1960. *Bull. Seismol. Soc. Amer.*, **50**, 81.
Pryce, M. H. L., 1953. *Advances in Physics*, **2**, 67.
Takeuchi, H., Press, F. & Kobayashi, N., 1959. *Bull. Seismol. Soc. Amer.*, **49**, 355.
Stoneley, R., 1953. *Bull. Seismol. Soc. Amer.*, **43**, 127.